Inorganic Chemistry
Article

Inorg. Chem. **2010**, *49*, 9217–9229 **9217**
DOI: 10.1021/ic100696r

Chemoselectivity Diversity in the Reaction of $LiNC_6F_5SiMe_3$ with Nitriles and the Synthesis, Structure, and Reactivity of Zirconium Mono- and Tris[2-(2-pyridyl)tetrafluorobenzimidazolate] Complexes

Sinai Aharonovich,[†] Mark Botoshansky,[†] Robert M. Waymouth,[‡] and Moris S. Eisen*[,†]

[†]*Schulich Faculty of Chemistry and Institute of Catalysis Science and Technology, Kyriat Hatechnion, Technion—Israel Institute of Technology, Haifa 32000, Israel, and* [‡]*Department of Chemistry, Stanford University, Stanford, California 94305-5080*

Received April 12, 2010

Unlike the reaction of $LiNTMS_2 \cdot TMEDA$ (TMS = $SiMe_3$; TMEDA = tetramethylethylenediamine) with 2-cyanopyridine, which results in the nearly exclusive formation of the amidinate, $(Me_3SiNC_6F_5)Li \cdot TMEDA$ (**1**) reacts with 2-cyanopyridine in toluene to yield quantitatively the lithium pyridyltetrafluorobenzimidazolate complex $[C_6F_4N_2C(2\text{-}C_5H_4N)]Li \cdot TMEDA$ (**3**). In this work, the reactivity of complex **1** toward aromatic nitriles Ar−CN (Ar = Ph, *o*-$OMeC_6H_4$, C_6F_5, 2-pyridyl) was examined. Whereas complex **1** fails to react with *o*-methoxybenzonitrile, its reaction with benzonitrile or pentafluorobenzonitrile gives triphenyl-1,3,5-triazine (**4**) or the hexacoordinate lithium polymer $[LiN(4\text{-}NCC_6F_4)(C_6F_5) \cdot THF \cdot TMEDA]_n$ (**7**), respectively. When **1** is reacted with 2-cyanopyridine in tetrahydrofuran (THF), the benzimidazolate coordination polymer $\{[C_6F_4N_2C(2\text{-}C_5H_4N)]Li \cdot THF\}_n$ (**5**) is obtained. Herein we discuss how this diverse chemoselectivity in the reaction of the examined lithium N-silylated amides $LiNRTMS \cdot TMEDA$ (R = TMS, C_6F_5) with nitriles is influenced by the electronic properties of the nitrile or amide substituents and by the ability of these substituents to interact with the lithium or silicon atoms. Further, we present the syntheses and structures of zirconium tris(pyridyltetrafluorobenzimidazolate) chloride (**10**) and zirconium bis(dimethylamido)(pyridyltetrafluorobenzimidazolate) chloride·THF (**11**) complexes. These complexes, the first prepared zirconium mono- and tris(benzimidazolate)s, were crystallographically characterized and examined in the polymerization of propylene with methyl aluminoxane (1:1000 Zr/Al molar ratio).

Introduction

Utilization of the amidinates $[N(R_1)C(R_2)NR_3]^-$ as ancillary ligands in the synthesis of coordination compounds[1,2] is partially due to their ability to form stable complexes of metals or metalloids from the s, p, d, and f blocks, which can support unusual bonding motifs and reactivities.[1−9] Lithium amidinates are widely used as ligand-transfer reagents in the preparation of the aforementioned amidinate complexes and as synthons in the preparation of various aza heterocycles[10−13] and other valuable organonitrogen compounds.[9,14,15] These applications have motivated, in the last 2 decades, substantial studies of the structural chemistry of these lithium complexes.

The structure of an amidinate complex, in general, can be influenced by three main structural factors: (i) the tautomeric form of the amidinate (Figure 1), (ii) the amidinate coordination mode (chelating or bridging; Figure 2a−d), and (iii) the degree and manner of participation of the amidinate π system in the bonding (compare part b with parts c and d in Figure 2). These structural factors can be influenced by the properties of other ligands in the coordination sphere,[2,11,15−22] by the electronic or steric properties of the amidinate backbone substituents,[2,7,11,13,16,20,21,23] or by the presence of pendant coordinating groups.[5,8,18,22]

Benzimidazolates, along with the free base benzimidazoles, are an important class of compounds with diverse pharmaceutical applications[25] and coordination chemistry.[11,26−29] The benzimidazolates, which can be regarded as amidinates "frozen" at the *Z*-syn tautomer, are different from the latter ligand type in their exclusive preference for the κ^1 coordination mode (Figure 2e).[29,30] With a lack of adequate donors, the second nitrogen atom can also coordinate to a

*To whom correspondence should be addressed. E-mail: chmoris@tx.technion.ac.il.

(1) (a) Edelmann, F. T. *Adv. Organomet. Chem.* **2008**, *57*, 183–352. (b) Edelmann, F. T. *Chem. Soc. Rev.* **2009**, *38*, 2253–2268. (c) Kissounko, D. A.; Zabalov, M. V.; Brusova, G. P.; Lemenovskii, D. A. *Russ. Chem. Rev.* **2006**, *75*, 351–374. (d) Schareina, T.; Kempe, R. Amido ligands in coordination chemistry. In *Synthetic methods of organometallic and inorganic chemistry*; Herrmann, W. A., Ed.; Thieme: Stuttgart, Germany, 2002; Vol. *10*, pp 1−41.

(2) Junk, P. C.; Cole, M. L. *Chem. Commun.* **2007**, 1579–1590.

Published on Web 09/21/2010

neighboring metal center, thus creating the fairly common $\kappa^1{:}\kappa^1$ bimetallic bridging coordination mode (Figure 2f),[31] which may lead to the formation of coordination polymers[32] or cage structures.[27,28]

As a part of our efforts toward the tailoring of the steric and electronic properties of diazaallyl ligands and, in particular, the introduction of fluorinated moieties on the ligand backbone close to the coordinated metal, we have recently disclosed[11] the reaction of $(Me_3SiNC_6F_5)Li\cdot TMEDA$ (**1**; TMS = $SiMe_3$; TMEDA = tetramethylethylenediamine) with 2-cyanopyridine in toluene, which gives, after the addition of lithium amide to the C≡N bond and a concomitant [1,3] silyl shift, the asymmetric amidinate product $[C_6F_5NC(2\text{-}C_5H_4N)\text{-}NTMS]Li\cdot TMEDA$ (**2**). This amidinate is unstable in solution and undergoes, through an amino−imide intermediate, a facile, room-temperature, silicon-assisted activation of the ortho C−F bond to yield quantitatively lithium pyridyltetrafluorobenzimidazolate $[C_6F_4N_2C(2\text{-}C_5H_4N)]Li\cdot TMEDA$ (**3**) and TMSF. In general, the lithium amino−imide intermediate is known to alternatively attack, besides the trimethylsilyl group or the perfluorinated ring, other electrophiles in the system, such as carbodiimide[9] or another molecule of the nitrile, which, in the latter case, results in the formation of 1,3,5-triazapentadienes[33,34] or 1,3,5-triazines.[12,13,33] The presence of functionalities such as an acidic hydrogen or an

(3) For selected recent examples, see: (a) Aharonovich, S.; Volkis, V.; Eisen, M. S. *Macromol. Symp.* **2007**, *260*, 165–171. (b) Boyd, D. A.; Crutchley, R. J.; Fanwicka, P. E.; Ren, T. *Inorg. Chem.* **2010**, *49*, 1322–1324. (c) Cotton, F. A.; Li, Z.; Murillo, C. A. *Inorg. Chem.* **2009**, *48*, 11847–11852. (d) Cotton, F. A.; Murillo, C. A.; Young, M. D.; Yu, R.; Zhao, Q. *Inorg. Chem.* **2008**, *47*, 219–229. (e) Donahue, J. P.; Murillo, C. A. *Dalton Trans.* **2008**, 1547–1551. (f) Evans, W. J.; Walensky, J. R.; Ziller, J. W. *Inorg. Chem.* **2010**, *49*, 1743–1749. (g) Evans, W. J.; Walensky, J. R.; Ziller, J. W. *Organometallics* **2010**, *29*, 101–107. (h) Ge, S.; Meetsma, A.; Hessen, B. *Organometallics* **2008**, *27*, 3131–3135. (i) Jones, C.; Rose, R. P.; Stasch, A. *Dalton Trans.* **2008**, 2871–2878. (j) Jones, C.; Schulten, C.; Rose, R. P.; Stasch, A.; Aldridge, S.; Woodul, W. D.; Murray, K. S.; Moubaraki, B.; Brynda, M.; La Macchia, G.; Gagliardi, L. *Angew. Chem., Int. Ed.* **2009**, *48*, 7406–7410. (k) Kondo, H.; Sue, T.; Kageyama, A.; Yamaguchi, Y.; Sunada, Y.; Nagashima, H. *J. Organomet. Chem.* **2009**, *694*, 795–800. (l) Luo, Y.; Wang, X.; Chen, J.; Luo, C.; Zhang, Y.; Yao, Y. *J. Organomet. Chem.* **2009**, *694*, 1289–1296. (m) Melgarejo, D. Y.; Chiarella, G. M.; Mohamed, A. A.; Fackler, J. P., Jr. *Z. Naturforsch., B: Chem. Sci.* **2009**, *64*, 1487–1490. (n) Pap, J. S.; DeBeer George, S.; Berry, J. F. *Angew. Chem., Int. Ed.* **2008**, *47*, 10102–10105. (o) Sciarone, T. J. J.; Nijhuis, C. A.; Meetsma, A.; Hessen, B. *Organometallics* **2008**, *27*, 2058–2065. (p) Sun, J.-F.; Chen, S.-J.; Duan, Y.; Li, Y.-Z.; Chen, X.-T.; Xue, Z.-L. *Organometallics* **2009**, *28*, 3088–3092. (q) Tsai, Y.-C.; Chen, H.-Z.; Chang, C.-C.; Yu, J.-S. K.; Lee, G.-H.; Wang, Y.; Kuo, T.-S. *J. Am. Chem. Soc.* **2009**, *131*, 12534–12535. (r) Wang, J.; Yao, Y.; Zhang, Y.; Shen, Q. *Inorg. Chem.* **2009**, *48*, 744–751. (s) Wu, Y.-Y.; Yeh, C.-W.; Chan, Z.-K.; Lin, C.-H.; Yang, C.-H.; Chen, J.-D.; Wang, J.-C. *J. Mol. Struct.* **2008**, *890*, 48–56.

(4) Aharonovich, S.; Botoshanski, M.; Tumanskii, B.; Nomura, K.; Waymouth, R. M.; Eisen, M. S. *J. Chem. Soc., Dalton Trans.* **2010**, *39*, 5643−5649.

(5) Bai, S.-D.; Tong, H.-B.; Guo, J.-P.; Zhou, M.-S.; Liu, D.-S.; Yuan, S.-F. *Polyhedron* **2010**, *29*, 262–269.

(6) Sen, S. S.; Jana, A.; Roesky, H. W.; Schulzke, C. *Angew. Chem., Int. Ed.* **2009**, *48*, 8536–8538.

(7) Heitmann, D.; Jones, C.; Mills, D. P.; Stasch, A. *Dalton Trans.* **2010**, *39*, 1877–1882.

(8) Rabinovich, E.; Aharonovich, S.; Botoshanski, M.; Eisen, M. S. *J. Chem. Soc., Dalton Trans.* **2010**, *39*, 6667−6676.

(9) Schmidt, S.; Gondzik, S.; Schulz, S.; Blaeser, D.; Boese, R. *Organometallics* **2009**, *28*, 4371–4376.

(10) (a) Boesveld, W. M.; Hitchcock, P. B.; Lappert, M. F. *J. Chem. Soc., Perkin Trans. 1* **2001**, 1103–1108. (b) Inukai, Y.; Oono, Y.; Sonoda, T.; Kobayashi, H. *Bull. Chem. Soc. Jpn.* **1979**, *52*, 516–520. (c) Knapp, C.; Lork, E.; Borrmann, T.; Stohrer, W.-D.; Mews, R. *Eur. J. Inorg. Chem.* **2003**, 3211–3220.

(11) Aharonovich, S.; Botoshanski, M.; Eisen, M. S. *Inorg. Chem.* **2009**, *48*, 5269–5278.

(12) Ma, Y.; Breslin, S.; Keresztes, I.; Lobkovsky, E.; Collum, D. B. *J. Org. Chem.* **2008**, *73*, 9610–9618.

(13) Volkis, V.; Nelkenbaum, E.; Lisovskii, A.; Hasson, G.; Semiat, R.; Kapon, M.; Botoshansky, M.; Eishen, Y.; Eisen, M. S. *J. Am. Chem. Soc.* **2003**, *125*, 2179–2194.

(14) Boesveld, W. M.; Hitchcock, P. B.; Lappert, M. F. *J. Chem. Soc., Dalton Trans.* **1999**, 4041–4046.

(15) Ong, T.-G.; O'Brien, J. S.; Korobkov, I.; Richeson, D. S. *Organometallics* **2006**, *25*, 4728–4730.

(16) (a) Aharonovich, S.; Kapon, M.; Botoshanski, M.; Eisen, M. S. *Organometallics* **2008**, *27*, 1869–1877. (b) Sanger, A. R. *Inorg. Nucl. Chem. Lett.* **1973**, *9*, 351–354.

(17) (a) Barker, J.; Barr, D.; Barnett, N. D. R.; Clegg, W.; Cragg-Hine, I.; Davidson, M. G.; Davies, R. P.; Hodgson, S. M.; Howard, J. A. K.; Kilner, M.; Lehmann, C. W.; Lopez-Solera, I.; Mulvey, R. E.; Raithby, P. R.; Snaith, R. *J. Chem. Soc., Dalton Trans.* **1997**, 951–955. (b) Cole, M. L.; Junk, P. C.; Louis, L. M. *J. Chem. Soc., Dalton Trans.* **2002**, 3906–3914. (c) Hitchcock, P. B.; Lappert, M. F.; Merle, P. G. *Phosphorus, Sulfur Silicon Relat. Elem.* **2001**, *168−169*, 363–366. (d) Hitchcock, P. B.; Lappert, M. F.; Merle, P. G. *Dalton Trans.* **2007**, 585–594. (e) Lisovskii, A.; Botoshansky, M.; Eisen, M. S. *J. Chem. Soc., Dalton Trans.* **2001**, 1692–1698. (f) Pang, X.-A.; Yao, Y.-M.; Wang, J.-F.; Sheng, H.-T.; Zhang, Y.; Shen, Q. *Chin. J. Chem .* **2005**, *23*, 1193–1197. (g) Richter, J.; Feiling, J.; Schmidt, H.-G.; Noltemeyer, M.; Brueser, W.; Edelmann, F. T. *Z. Anorg. Allg. Chem.* **2004**, *630*, 1269–1275. (h) Schmidt, J. A. R.; Arnold, J. *J. Chem. Soc., Dalton Trans.* **2002**, 3454–3461. (i) Stalke, D.; Wedler, M.; Edelmann, F. T. *J. Organomet. Chem.* **1992**, *431*, C1–C5. (j) Trifonov, A. A.; Lyubov, D. M.; Fedorova, E. A.; Fukin, G. K.; Schumann, H.; Muhle, S.; Hummert, M.; Bochkarev, M. N. *Eur. J. Inorg. Chem.* **2006**, 747–756. (k) Villiers, C.; Thuery, P.; Ephritikhine, M. *Eur. J. Inorg. Chem.* **2004**, 4624–4632.

(18) Aharonovich, S.; Botoshanski, M.; Rabinovich, Z.; Waymouth, R. M.; Eisen, M. S. *Inorg. Chem.* **2010**, *49*, 1220−1229.

(19) Baldamus, J.; Berghof, C.; Cole, M. L.; Hey-Hawkins, E.; Junk, P. C.; Louis, L. M. *Eur. J. Inorg. Chem.* **2002**, 2878–2884.

(20) Eisen, M. S.; Kapon, M. *J. Chem. Soc., Dalton Trans.* **1994**, 3507–3510.

(21) Knapp, C.; Lork, E.; Watson, P. G.; Mews, R. *Inorg. Chem.* **2002**, *41*, 2014–2025.

(22) (a) Bai, S.-D.; Tong, H.-B.; Guo, J.-P.; Zhou, M.-S.; Liu, D.-S. *Inorg. Chim. Acta* **2009**, *362*, 1143–1148. (b) Otero, A.; Fernandez-Baeza, J.; Antinolo, A.; Tejeda, J.; Lara-Sanchez, A.; Sanchez-Barba, L. F.; Lopez-Solera, I.; Rodriguez, A. M. *Inorg. Chem.* **2007**, *46*, 1760–1770.

(23) Baker, R. J.; Jones, C. *J. Organomet. Chem.* **2006**, *691*, 65–71.

(24) The nomenclature of the amidinate isomers/tautomers is adopted from: Patai, S.; Rappoport, Z. *The chemistry of amidines and imidates*; Wiley: Chichester, U.K., 1991.

(25) For selected recent reviews, see: (a) Bhattacharya, S.; Chaudhuri, P. *Curr. Med. Chem.* **2008**, *15*, 1762–1777. (b) Boiani, M.; Gonzalez, M. *Coord. Chem. Rev.* **2005**, *5*, 409–424. (c) Velik, J.; Baliharova, V.; Fink-Gremmels, J.; Bull, S.; Lamka, J.; Skalova, L. *Res. Vet. Sci.* **2004**, *76*, 95–108.

(26) (a) Chan, W. K. *Coord. Chem. Rev.* **2007**, *251*, 2104–2118. (b) Haga, M. *Compr. Coord. Chem. II* **2004**, *1*, 125–134. (c) Liu, S.; Zuo, W.; Zhang, S.; Hao, P.; Wang, D.; Sun, W.-H. *J. Polym. Sci., Part A: Polym. Chem.* **2008**, *46*, 3411–3423. (d) Lyaskovskyy, V. V.; Voitenko, Z. V.; Kovtunenko, V. A. *Chem. Heterocycl. Compd.* **2007**, *43*, 253–276. (e) Sun, W.-H.; Liu, S.; Zhang, W.; Zeng, Y.; Wang, D.; Liang, T. *Organometallics* **2010**, *29*, 732–741. (f) Tellez, F.; Lopez-Sandoval, H.; Castillo-Blum, S. E.; Barba-Behrens, N. *ARKIVOC* **2008**, *5*, 245–275.

(27) Banerjee, R.; Phan, A.; Wang, B.; Knobler, C.; Furukawa, H.; O'Keeffe, M.; Yaghi, O. M. *Science* **2008**, *319*, 939–943.

(28) Wang, B.; Cote, A. P.; Furukawa, H.; O'Keeffe, M.; Yaghi, O. M. *Nature* **2008**, *453*, 207–211.

(29) Berding, J.; van Dijkman, T. F.; Lutz, M.; Spek, A. L.; Bouwman, E. *Dalton Trans.* **2009**, 6948–6955.

(30) (a) Liang, B.; Wang, L.; Zhu, X.; Shi, H.; Peng, J.; Cao, Y. *J. Organomet. Chem.* **2009**, *694*, 3172–3178. (b) Bai, X.-Q.; Zhang, S.-H. *Acta Crystallogr., Sect. C: Cryst. Struct. Commun.* **2009**, *E65*, m397. (c) Zhang, S. H.; Zeng, M. H.; Liang, H. *Acta Crystallogr., Sect. C: Cryst. Struct. Commun.* **2007**, *E63*, m1055–m1056. (d) Panasyuk, A. G.; Aliev, Z. G.; Ranskii, A. N. *Russ. J. Coord. Chem.* **2006**, *32*, 266–269. (e) Chen, T.-R.; Chien, R.-H.; Yeh, A.; Chen, J.-D. *J. Organomet. Chem.* **2006**, *691*, 1998–2004.

(31) (a) Wu, T.; Li, D.; Feng, X.-L.; Cai, J.-W. *Inorg. Chem. Commun.* **2003**, *6*, 886–890. (b) Plass, W.; Pohlmann, A.; Subramanian, P. S.; Srinivas, D. *Z. Anorg. Allg. Chem.* **2002**, *628*, 1377–1384. (c) Yang, H.; Shi, J.; Chen, L.; Luo, B. *Polyhedron* **1996**, *15*, 3891–3895. (d) Pellinghelli, M. A.; Tiripicchio, A.; Cabeza, J. A.; Oro, L. A. *J. Chem. Soc., Dalton Trans.* **1990**, 1509–1512. (e) Beardwood, P.; Gibson, J. F. *J. Chem. Soc., Chem. Commun.* **1986**, 490–492. (f) Kolks, G.; Lippard, S. J. *Acta Crystallogr., Sect. C: Cryst. Struct. Commun.* **1984**, *C40*, 261–271.

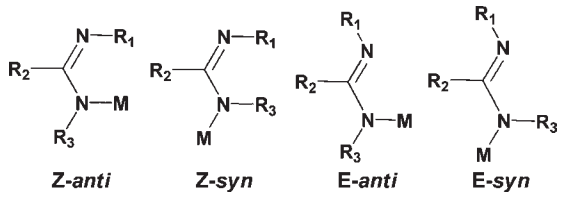

Figure 1. Structures and accepted nomenclatures of the amidinate tautomeric forms.[24]

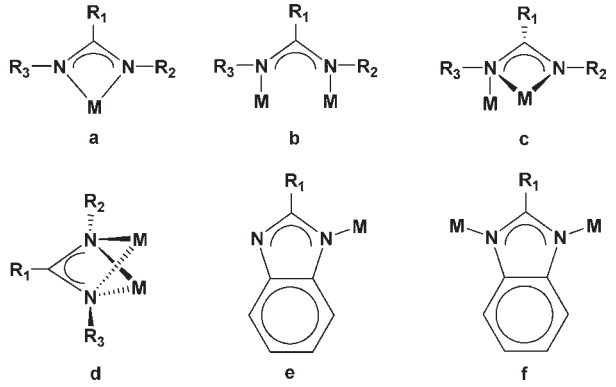

Figure 2. Examples of common coordination modes of the *E*-anti amidinate (a−d) and benzimidazolate (e and f) ligands: (a) κ^2 and (b) κ^1:κ^1 bimetallic bridging; (c) κ^2:κ^1 bimetallic bridging and monochelating; (d) κ^2:κ^2 bimetallic bridging and bischelating; (e) κ^1 and (f) κ^1:κ^1 bimetallic bridging.

electrophilic aromatic ring may induce competing deprotonation or nucleophilic aromatic substitution reactions with either the amino−imide moiety or the parent lithium amide.[35] The many possible reaction paths raise fundamental questions regarding the effect of the electronic properties of the nitrile and amide and the coordination mode of the lithium metal in the reaction between nitriles and N-silylated amides.

In the first part of the current presentation, we compare the reactions of complex **1** and $LiNTMS_2 \cdot TMEDA$ with several substituted aromatic nitriles of similar steric properties and we demonstrate how the electronic properties of the nitrile and amide and the presence of pendant groups that can participate in the coordination of lithium or silicon influence the chemoselectivity of the reaction. In addition, we present the synthesis and structure of a lithium coordination polymer of the pyridyltetrafluorobenzimidazolate ligand and also the synthesis and structure of a unique hexacoordinate lithium coordination polymer with TMEDA, tetrahydrofuran (THF), and nonafluoro-*p*-benzonitrilephenylamide ligands.

In the second part of the presentation, we disclose the syntheses, reactivity, structure, and propylene polymerization behavior of the zirconium mono- and tris[tetrafluoro-2-(2-pyridyl)benzimidazolate] complexes, which are, to the best of our knowledge, the first synthesized zirconium mono- and tris(benzimidazolate)s.

Results and Discussion

Reactivity of 1 toward Nitriles. Reaction of Complex 1 with Benzonitrile and *o*-Methoxybenzonitrile. When benzonitrile is added to a cold toluene solution (0 °C) of complex **1**, the color of the solution changes from yellow to dark purple-blue after the reaction mixture is brought to room temperature. From this solution, crystals of triphenyl-1,3,5-triazine (**4**), which was characterized using ^{1}H NMR and X-ray analysis, can be obtained in an isolated yield of 67% (Scheme 1). Because the trimerization of nitriles by metal amides involves amino−imide and 1,3,5-triazahexatriene intermediates[12] (Scheme 2), it seems that, while the nucleophilic addition of complex **1** to benzonitrile is operative, the second nucleophilic attacks on silicon or on the perfluorinated ring are slower than an attack on another nitrile molecule, unlike the situation in the reaction of complex **1** and 2-cyanopyridine[11] or in the reaction of $LiNTMS_2 \cdot TMEDA$ and 2-cyanopyridine[16a] or benzonitrile.[36]

When a similar reaction between complex **1** and *o*-methoxybenzonitrile is attempted, no significant color change was noted, and the starting materials could be identified (via ^{1}H NMR) as the major components of the mixture even after prolonged reaction times (Scheme 1). This result implies that in the case of *o*-methoxybenzonitrile even the first nucleophilic addition is hindered, which again is in a sharp contrast to the situation for the reaction of this nitrile and $LiNTMS_2 \cdot TMEDA$, which provides bis(trimethylsilyl)amidinate in good yields.[16a]

Reaction of Complex 1 with 2-Cyanopyridine in THF. When the addition−elimination reaction of 2-cyanopyridine with complex **1** is performed in THF, transparent crystals of the polymeric lithium benzimidazolate·THF complex **5** can be obtained in 78% isolated yield by the slow evaporation of the solvent (Scheme 3). As was mentioned in the Introduction, when a similar reaction is carried out in toluene, the benzamidinate **2** and its cyclization product, the benzimidazolate **3**, are produced (Scheme 3).[11] The solubility of **5** in THF suggests that upon polymer solvation fragments of smaller lithium benzimidazolate monomers, such as a 2THF complex (**6**, Scheme 3), are obtained. Polymer **5** was also obtained when a THF solution of complex **3** was vacuum-concentrated. We have recently reported the formation of coordination polymers of 3- and 4-pyridylamidinates, which resulted from the coordination of lithium centers to the pendant nitrogen atoms at the expense of TMEDA.[18] The displacement of TMEDA with THF in complex **3** is also supported by the almost identical ^{1}H and ^{19}F NMR spectra (pyridyl and tetrafluorophenylene regions, respectively) of **3** and **5** in THF-d_8.

Unlike the four signals in the room-temperature ^{19}F NMR spectrum of **3** in toluene-d_8, which support the

(32) (a) Li, X.-M. *Acta Crystallogr., Sect. C: Cryst. Struct. Commun.* **2007**, *E63*, m1984. (b) Huang, X. C.; Luo, W.; Shen, Y. F.; Ng, S. W. *Acta Crystallogr., Sect. C: Cryst. Struct. Commun.* **2007**, *E63*, m2041. (c) Cui, Y.-C.; Wang, J. u.; Liu, B.; Gao, G.-G.; Wang, Q.-W. *Acta Crystallogr., Sect. C: Cryst. Struct. Commun.* **2007**, *E63*, m1204–m1205. (d) Zeng, M. H.; Shen, X. C.; Ng, S. W. *Acta Crystallogr., Sect. C: Cryst. Struct. Commun.* **2006**, *E62*, m2194–m2195. (e) Xu, H.-J.; Liu, Y.-X.; Shen, Z.; Tian, Y.-Q.; You, X.-Z. *Z. Anorg. Allg. Chem.* **2005**, *631*, 1349–1351. (f) Sanchez, V.; Storr, A.; Thompson, R. C. *Can. J. Chem.* **2002**, *80*, 133–140.

(33) (a) Zhou, M.; Song, Y.; Gong, T.; Tong, H.; Guo, J.; Weng, L.; Liu, D. *Inorg. Chem.* **2008**, *47*, 6692–6700. (b) Cui, D.; Nishimura, M.; Hou, Z. *Angew. Chem., Int. Ed.* **2005**, *44*, 959–962.

(34) (a) Guo, J.-P.; Wong, W.-K.; Wong, W.-Y. *Eur. J. Inorg. Chem.* **2006**, 3634–3640. (b) Guo, J.; Wong, W.-K.; Wong, W.-Y. *Eur. J. Inorg. Chem.* **2004**, 267–275.

(35) (a) Divald, S.; Chun, M. C.; Joullie, M. M. *J. Org. Chem.* **1976**, *41*, 2835–2846. (b) Bures, E.; Nieman, J.; Yu, A. S.; Spinazze, P. G.; Bontront, J.-L. J.; Hunt, I. R.; Rauk, A.; Keay, B. A. *J. Org. Chem.* **1997**, *62*, 8750–8759.

(36) Wedler, M.; Knoesel, F.; Noltemeyer, M.; Edelmann, F. T.; Behrens, U. *J. Organomet. Chem.* **1990**, *388*, 21–45.

Scheme 1. Reactivity of the Lithium *N*-(Trimethylsilyl)pentafluoroanilide Complex **1** with Benzonitrile and *o*-Methoxybenzonitrile

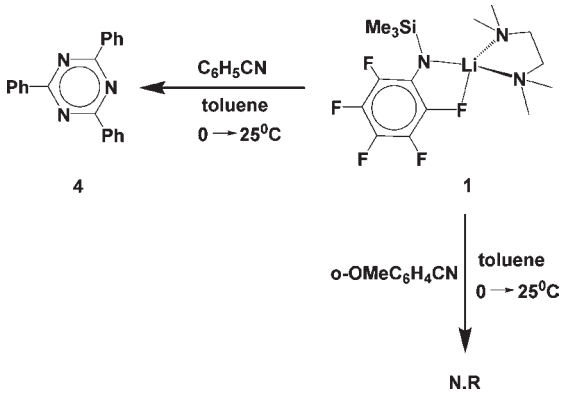

Scheme 2. Plausible Mechanism for the Trimerization of Nitriles by Lithium Amides

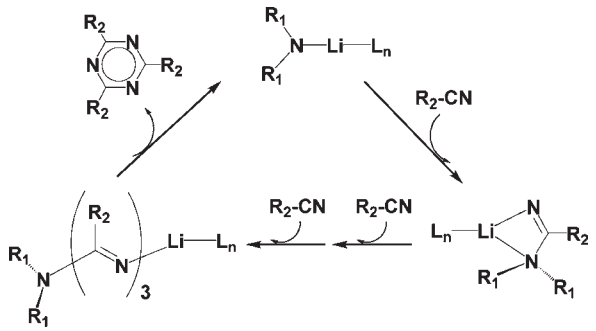

retention of its solid-state structure in solution at these conditions, there are only two fluorine signals in the ^{19}F NMR spectrum of **3** in THF-d_8.[11] This higher symmetry about the tetrafluorinated ring (AB pattern) implies that a rapid rotation of the pyridine ring and Li−N(imidazolate) bond breaking and formation are operative.

Crystallographic data and structure refinement details for complex **5** and selected bond lengths and angles are presented in Tables 1 and 2, respectively. In the crystalline lattice of complex **5** (Figure 3a), each lithium atom has a distorted tetrahedral environment with two coordination sites occupied by the κ^2-chelating NCCN unit of the 2-(2-pyridyl)tetrafluorobenzimidazolate ligand. The two other coordination sites are taken by a THF oxygen atom and a second nitrogen atom of an adjacent benzimidazolate fragment (κ^1:κ^1 bimetallic bridging benzimidazolate coordination mode). The lithium benzimidazolate Li−N3 bond [2.083(4) Å] is slightly longer than the Li−N2 bond [2.028(4) Å].

The long distance (3.033 Å) between the lithium atom and the *o*-fluorine F1 atom implies that only a weak Coulombic attraction may exist between these atoms. The crystal lattice is composed of infinite chains made by the bridging benzimidazolate ligands and lithium atoms, whereas the THF ligands are disposed in a quasi-syndiotactic arrangement. Counterintuitively, the tetrafluoro and pyridyl rings of the 2-(2-pyridyl)tetrafluorobenzimidazolate ligand point to the same direction of the chain rather than adopting an alternating stereoarrangement, which is expected to provide less steric and Coulombic repulsion between adjacent rings. This orientation probably results from π stacking between the pyridyl and tetrafluoeophenylene ring of neighboring chains (Figure 3b), which create a two-dimensional supramolecular structure (the pyridyl−tetrafluorophenylene centroid distance is 3.906 Å).

Scheme 3. Reactivity of the Lithium *N*-(Trimethylsilyl)pentafluoroanilide Complex **1** with 2-Cyanopyridine in THF and Toluene

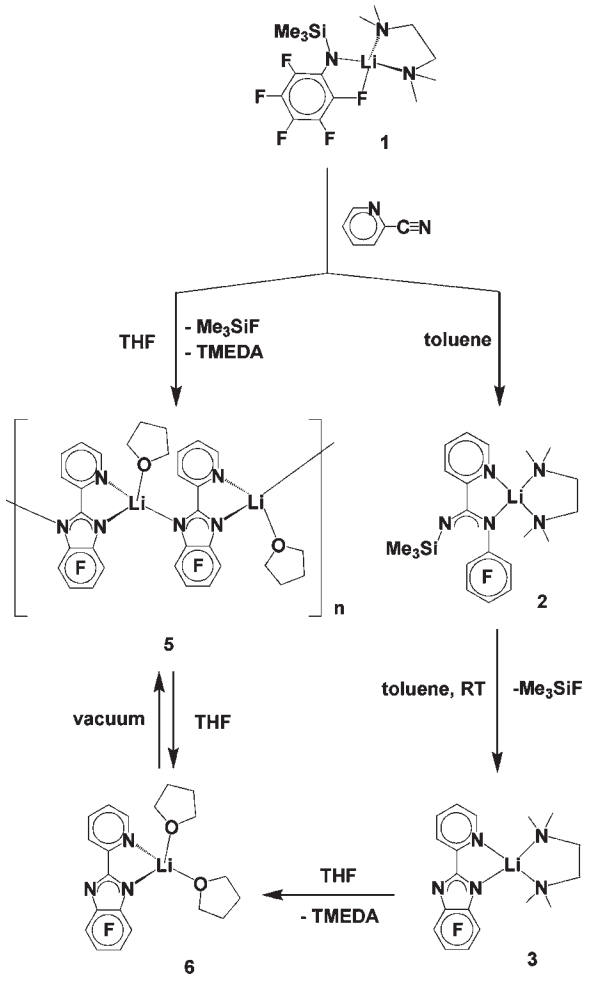

Reaction of Complex 1 with Pentafluorobenzonitrile. In an attempt to synthesize the perfluorinated 2-phenylbenzimidazolate ligand, we have examined the reaction of complex **1** with pentafluorobenzonitrile. When a similar reaction is performed with $LiNTMS_2$, the chemoselectivity of the nucleophilic attack (on the nitrile carbon or para position of the perfluorinated ring) is dependent on the solvent. Thus, when the reaction is carried out in ether,[21] the pentafluoroamidinate is formed, whereas the reaction of the same starting materials in THF[37] gives a mixture of two para substitution products (see eqs 1 and 2, respectively). These substitution products, *p*-*N*,*N*-bis(trimethylsilyl)aminotetrafluorobenzonitrile and the coordination polymer {lithium [bis(4-cyano-2,3,5,6-tetrafluorophenyl)amide]·2THF}$_n$, result from LiF or Me_3SiF elimination, respectively.

$$LiNTMS_2 + C_6F_5CN \xrightarrow[\text{ether}]{} [C_6F_5C(NTMS)_2Li\cdot Et_2O]_2 \quad (1)$$

(37) Shmulinson, M.; Pilz, A.; Eisen, M. S. *J. Chem. Soc., Dalton Trans.* **1997**, 2483–2486.

Table 1. Crystallographic Data for Complexes **5**, **7**, **10**, and **11**

	5	**7**	**10**	**11**
empirical formula	$C_{16}H_{12}F_4LiN_3O$	$C_{23}H_{24}F_9LiN_4O$	$C_{43}H_{20}ZrN_9F_{12}Cl$	$C_{20}H_{24}ZrN_5F_4ClO$
fw [g/mol]	345.23	550.40	1017.35	553.11
T [K]	240(2)	240(2)	240.0(2)	293(2)
λ [Å]	0.710 73	0.710 73	0.710 73	0.710 73
cryst syst	orthorhombic	monoclinic	monoclinic	monoclinic
space group	*Pbca*	$P2_1$	$P2_1/c$	$C2/c$
a [Å]	15.886(3)	8.807(2)	12.048(2)	11.225(2)
b [Å]	11.780(2)	16.647(3)	23.408(5)	15.239(3)
c [Å]	16.277(3)	9.424(2)	15.806(3)	27.853(6)
β [deg]	90	114.82(3)	116.72(3)	98.972(3)
V [Å^3]	3046.0(3)	1254.0(5)	3981(1)	4706.2(16)
Z	8	2	4	8
ρ [g/cm^3]	1.506	1.468	1.697	1.561
μ(Mo Kα) [mm^{-1}]	0.129	0.140	0.447	0.634
R1, wR2 [$I > 2\sigma(I)$]	0.0418, 0.0935	0.0411, 0.1107	0.0571, 0.1445	0.0674, 0.1770
R1, wR2 (all data)	0.0783, 0.1039	0.0576, 0.1186	0.1100, 0.1683	0.1624, 0.2031
GOF on F^2	0.929	1.031	1.032	1.051
F(000)	1408	256	2024	2240
θ range for data collection [deg]	2.49−25.02	2.38−25.41	1.89−25.63	2.27−25.01
limiting indices	$-16 \le h \le 18$	$0 \le h \le 10$	$0 \le h \le 14$	$0 \le h \le 13$
	$-13 \le k \le 14$	$0 \le k \le 20$	$-28 \le k \le 0$	$0 \le k \le 17$
	$-17 \le l \le 19$	$-11 \le l \le 10$	$-19 \le l \le 16$	$-33 \le l \le 32$
reflns collected/unique	15 200/2679	8173/2390	26 405/7378	27 004/4010
R(int)	0.0869	0.0430	0.0690	0.0970
completeness to θ_{max} [%]	100.0	99.6	98.1	96.7
data/restraints/parameters	2679/0/226	2390/1/347	7378/0/567	4010/0/274
largest diff peak and hole [e/Å^3]	0.165 and 0.191	0.210 and −0.183	0.675 and −0.568	0.579 and −0.731

Table 2. Selected Bond Lengths [Å] and Angles [deg] for Complex **5**

Bond Lengths

N1−Li1	2.140(4)	O1−Li1	1.962(3)	N2−C2	1.367(3)
N2−Li1	2.028(4)	N2−C1	1.344(2)	N3−C3	1.387(3)
N3−Li1	2.083(4)	N3−C1	1.359(2)	C1−C8	1.475(3)

Bond and Torsion Angles

N2−C1−N3	116.83(18)	N2−Li1−N1	80.04(13)
O1−Li1−N2	102.35(15)	N3−Li1−N1	113.56(16)
O1−Li1−N3	104.12(16)	N2−C1−C8−N1	0.06
N2−Li1−N3	137.13(19)	Li1−N2−C1−C8	1.23
O1−Li1−N1	120.13(18)	Li1−N3−C1−C8	10.69

$$LiNTMS_2 + C_6F_5CN \xrightarrow[THF]{} p\text{-}TMS_2NC_6F_4CN + [(p\text{-}NCC_6F_4)_2NLi\cdot 2THF]_n \quad (2)$$

Hence, when pentafluorobenzonitrile is added to a chilled THF solution of complex **1**, the bright-yellow color of the reaction mixture is changed to mustard-yellow, and the coordination polymer {lithium [(4-cyano-2,3,5,6-tetrafluorophenyl)(pentafluorophenyl)amide]·THF·TMEDA}$_n$ (**7**) can be isolated from the solution in 87% yield as faint-yellow crystals (Scheme 4).

Contrarily to the reaction with $LiNTMS_2$, this Me_3SiF elimination product, which results from a silicon-assisted SN_{AR} reaction, is not accompanied by *N*-(trimethylsilyl)-*N*-(4-cyano-2,3,5,6-tetrafluorophenyl)pentafluoroaniline (**8**), the expected product from LiF elimination. When lithium (pentafluorophenyl)(trimethylsilyl)amide (**9**)[11] in ether was used, no benzamidinate product was obtained;[21] however, when THF and TMEDA (1 equiv) were added to the reaction mixture, polymer **7** was produced. The high chemoselectivity of complex **1** toward the production of polymer **7** is plausibly due to its lower reactivity toward nucleophilic attack reactions in comparison to $LiNTMS_2$ and implies that, under the examined reaction conditions, the aromatic para position of pentafluorobenzonitrile is more susceptible to nucleophilic attack than the nitrile carbon. Concerning the heavier halogens, the rate-determining step of the nucleophilic aromatic substitution is usually the σ-complex formation;[38a] however, in fluoroaromatic substrates, the rate-determining step can often be the fluoride elimination[38b] because of the exceptionally high enthalpy of the C−F bond.[38c] This involvement of the fluoride elimination step in the kinetics of the rate-determining step was, e.g., observed in the reaction of 2,4-dinitrofluorobenzene (Sanger's reagent) with *N*-methylaniline.[38d] Therefore, C−F bond activation by coordination of the fluorine atom is expected to accelerate the reaction in such cases. Because the Si−F bond enthalpy is more than 100 kJ greater than that of the Li−F bond,[37] the formation of a Si−F interaction is expected to provide a more significant activation of the C−F bond in the transition state than that of a Li−F interaction, and thus silicon is expected to lower the relevant activation barrier more efficiently than lithium. This difference in activation barriers, which translates to the observed selectivity, is more noticeable with the less reactive, weaker nucleophile **1**.

Crystallographic data and structure refinement details for complex **7** and selected bond lengths and angles are presented in Tables 1 and 3, respectively. In the solid state (Figure 4), complex **7** is a linear coordination polymer. The repeating units of **7** consist of a distorted octahedral

(38) (a) Smith, M. B.; March, J. *March's advanced organic chemistry: reactions, mechanism and structure*, 5th ed.; Wiley-Interscience: New York, 2007; pp 854−857. (b) Nudelman, N. S. In *The Chemistry of Amino, Nitroso, Nitro and Related Groups*; Patai, S., Ed.; Wiley: Chichester, U.K., 1996; pp 1215−1300. (c) O'Hagan, D. *Chem. Soc. Rev.* **2008**, *37*, 308–319. (d) De La Mare, P. B. D.; Swedlund, B. E. Heterolytic Mechanisms of Substitution Involving Carbon-Halogen Bonds. In *The Chemistry of the Carbon−Halogen Bond*; Patai, S., Ed.; Wiley: New York, 1973; pp 472−475 and references cited therein.

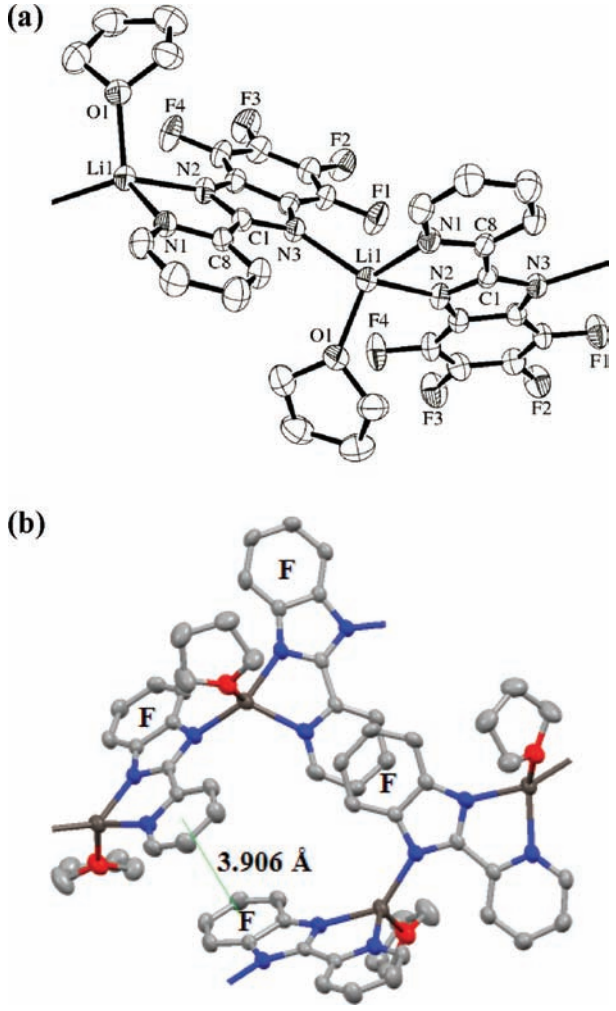

Figure 3. (a) ORTEP diagram of the molecular structure of a repeating unit of polymer **5** (50% thermal ellipsoids), showing the mutual arrangement of the fluorinated 2-(2-pyridyl)benzimidazolate ligands and the quasi-syndiotactic stereochemistry of the THF ligands at the lithium centers. Hydrogen atoms are omitted for clarity. (b) Illustration of the segments of two neighboring chains of polymer **5** (50% thermal ellipsoids), showing the π-stacking interactions. Hydrogen and fluorine atoms are omitted for clarity (the tetrafluorophenylene ring is marked with an "F").

lithium atom, which is cis-bischelated by an NCCF fragment from a 4-cyano-2,3,5,6-tetrafluorophenyl ring, and a TMEDA ligand.

The LiNCCF metallacycle is virtually planar, and contrarily to complex **1**, no C−F bond elongation is noted, as shown by the similarity of the C2−F1 and C6−F4 bond lengths [1.358(4) and 1.362(4) Å, respectively]. The two remaining coordination sites are taken by a THF molecule and a nitrile nitrogen atom from an adjacent repeating unit. Whereas coordination polymers[39] of hexacoordinate lithium are extremely rare by their own right,[40] complex **7** is, to the best of our knowledge, the first hexacoordinate lithium coordination polymer with both TMEDA and THF ligands.

The bond lengths of all of the ligands in polymer **7** to the lithium atom are markedly longer in comparison to bonds of similar ligands to lithium in less saturated complexes, as suggested by a search of the Cambridge Crystallographic Data Centre (CCDC).[41]

Interestingly, the Li−N_{CN} bond length in complex **7** [2.142(8) Å] is even shorter than the Li−amide bond length [2.209(7) Å], suggesting an extensive delocalization of the negative charge from the amide to the nitrile, which is supported by the partly quinonical 4-cyano-2,3,5,6-tetrafluorophenylamide ring (Table 3). The hexacoordination of the lithium atom is probably facilitated by the soft nature of the 4-cyano-2,3,5,6-tetrafluorophenyl-(pentafluorophenyl)amide ligand, whereas the polymerization is aided by the "two-faced" 1,4 distribution of the negative charge in this ligand.

Insights into the Reactions of Complex 1 or LiNTMS$_2$·TMEDA with Nitriles. When LiNTMS$_2$·TMEDA is added to 2-cyanopyridine or benzonitrile (route i or ii, respectively, Scheme 5), the imido nitrogen atom of the generated bis-silylated amino−imide (**A** or **E**, respectively, Scheme 5) can attack either a silicon atom (rendering the 1,3 silyl shift) or another nitrile molecule (toward the nitrile trimerization; Scheme 2). The production of the bis-silylated amidinates (**D** and **H**) in high yields from these two nitriles and also from *o*-methoxybenzonitrile[16] suggests that the 1,3-shift reaction is faster in these cases, as implied by the production of triazine when dialkylamides are used.[16b]

Because the silyl shift proceeds through a concerted four-membered transition state (**C** and **G**, Scheme 5),[43,44] we propose that a preliminary condition to its occurrence is the coordination of the lithium trans to the amino nitrogen atom about the imido C=N bond (as presented in species **B** and **F**). This κ^1 amino−imide coordination mode is expected to be less favored enthalpically than the κ^2 mode, if no significant pendant donors are present. The 2-pyridyl substituent can, therefore, provide a better stabilization of this κ^1 amino−imide in comparison to the weaker Li−aryl π interactions provided by the phenyl ring (compare **B** to **F**). Similar preference for the formation of such NCCN chelates in the 2-pyridylamidinate ligand is given in the structure of complex **3**,[11] in the catalytic propylene polymerization by the titanium bis-(2-pyridyl)amidinate complex,[45] and in the precise cyclo-oligomerization of ε-caprolactone by the thorium bis-(2-pyridyl) complex.[8] This lithium chelation, besides clearing the way for the silyl shift,[44] is also expected to increase the nucleophilicity of the imide.

The different reactivities of amide **1** with 2-cyanopyridine or benzonitrile (routes iii or iv, respectively) are particularly obvious when compared to the exclusive amidinate formation with LiNTMS$_2$·TMEDA. The

(39) Fromm, K. M. *Coord. Chem. Rev.* **2008**, *252*, 856–885.
(40) (a) Henderson, W. A.; Brooks, N. R.; Young, V. G., Jr. *J. Am. Chem. Soc.* **2003**, *125*, 12098–12099. (b) Liu, X.; Guo, G.-C.; Wu, A. Q.; Huang, J.-S. *Inorg. Chem. Commun.* **2004**, *7*, 1261–1263.
(41) For the Cambridge Crystallographic Data Centre (CCDC), see http://www.ccdc.cam.ac.uk/
(42) Hansch, C.; Leo, A.; Hoekman, D. *Exploring QSAR: Hydrophobic, Electronic, and Steric Constants*; American Chemical Society: Washington, DC, 1995; pp 254 and 270.
(43) (a) Takahashi, M.; Kira, M. *J. Am. Chem. Soc.* **1999**, *121*, 8597–8603. (b) Jia, Z.; Feng, S.; Song, E.; Sun, W.; Cong, L. *Int. J. Quantum Chem.* **2008**, *109*, 342–348.
(44) Lim, C.; Lee, H. S.; Kwak, Y.-W.; Choi, C. H. *J. Comput. Chem.* **2006**, *27*, 228–237.
(45) Aharonovich, S.; Kapon, M.; Botoshanski, M.; Eisen, M. S. Substituent Effects in Propylene Polymerization Promoted by Titanium(IV) Amidinates. *Proceedings of the 38th International Conference on Coordination Chemistry*, Kenes International, Jerusalem, Israel, July 20−25, 2008; p 369.

Scheme 4. Reactivity of the Lithium *N*-(Trimethylsilyl)pentafluoroanilide·TMEDA Complex **1** or the Unsolvated Lithium *N*-(Trimethylsilyl)-pentafluoroanilide **9** with Pentafluorobenzonitrile in THF and Ether, Respectively

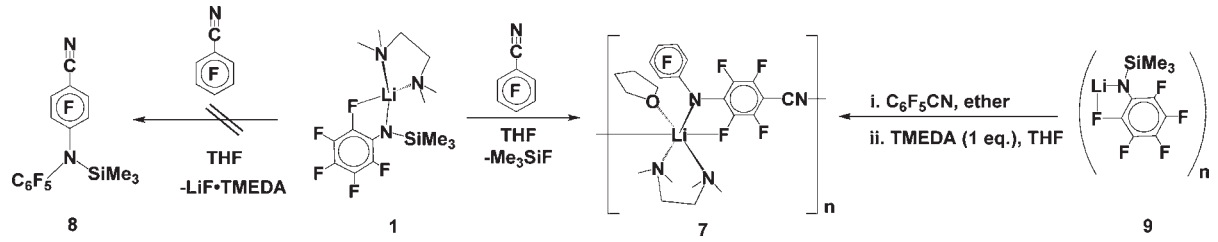

Table 3. Selected Bond Lengths [Å] and Angles [deg] for Complex **7**

Bond Lengths

F1−C2	1.358(4)	N1−Li1	2.209(7)	C1−C2	1.417(5)
F1−Li1	2.309(7)	N2−C23	1.146(5)	C2−C3	1.358(5)
F4−C6	1.362(4)	N2−Li1	2.142(8)	C3−C4	1.402(6)
O1−Li1	2.232(8)	N3−Li1	2.310(7)	C4−C5	1.403(5)
N1−C1	1.336(5)	N4−Li1	2.357(8)	C4−C23	1.416(5)
N1−C7	1.395(5)	C1−C6	1.417(5)	C5−C6	1.354(5)

Bond and Torsion Angles

C1−N1−C7	119.6(3)	N1−Li1−N4	98.2(3)
C1−N1−Li1	118.4(3)	O1−Li1−N4	165.6(4)
C7−N1−Li1	119.6(3)	N3−Li1−N4	78.7(2)
C23−N2−Li1	168.9(4)	F1−Li1−N4	85.3(2)
C2−F1−Li1	114.3(3)	O1−Li1−N3	89.2(3)
N2−C23−C4	177.3(4)	N2−Li1−F1	170.7(4)
N2−Li1−N1	98.5(3)	N1−Li1−F1	72.2(2)
N2−Li1−O1	93.4(3)	O1−Li1−F1	87.1(3)
N1−Li1−O1	91.1(3)	N3−Li1−F1	91.0(3)
N2−Li1−N3	98.3(3)	Li−N1−C1−C2	3.78
N1−Li1−N3	163.1(4)	N1−C1−C2−F1	4.42
N2−Li1−N4	96.1(3)		

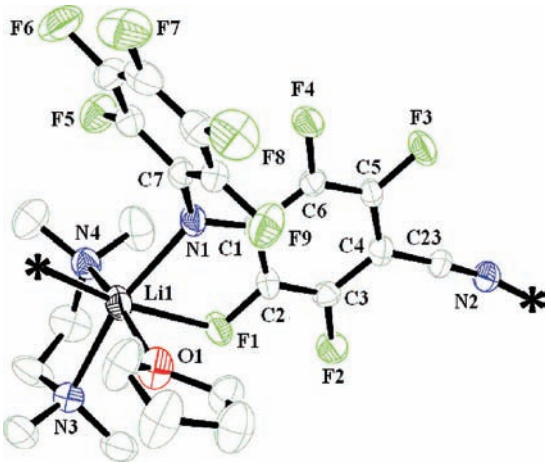

Figure 4. ORTEP diagram of the molecular structure of the repeating unit of polymer **7** (50% thermal ellipsoids). Hydrogen atoms are omitted for clarity.

amino−imide complex generated by **1** (complexes **I** and **N**) can participate in an additional reaction: the intramolecular attack of the ortho position of the *N*-pentafluoroaryl ring. Similarly to the silyl shift, this reaction is also expected to proceed in a κ^1-bonded amino−imide (complexes **K** and **O**). Therefore, the formation of both amidinate and benzimidazolate in the reaction of **1** with 2-cyanopyridine suggests that the amino−imide **I** can isomerizes to either species **J** or **L**, in which attack on the silicon or on the ortho position of the perfluorinated ring results in the formation of the amidinate **2** or the benzimidazolate **3**, respectively. The triazine formation (**4**) by the reaction of **1** with benzonitrile suggests, therefore, that the isomerization, or more probably, the attack of the imide is effectively suppressed in this system, allowing the slower nitrile trimerization to prevail (route iv, Scheme 5). Therefore, the lack of reactivity of amide **1** with *o*-methoxybenzonitrile hints that the amino−imide intermediate is not formed in this case.

These observations indicate that the *N*-pentafluoro substituent has an inhibiting effect on the TMS shift whereas the 2-pyridyl carbon substituent has an accelerating effect and that the effect of the latter is stronger. The major causes for these effects are not simply the steric bulk of the substituents, due to the similar steric properties of the phenyl and pyridyl rings, the TMS and C_6F_5 moieties, and the OMe and F substituents.[42] Except for the latter case, the expected electronic effects of these substituents on the reaction rates are opposite to the experimental observations: Replacement of the phenyl ring by the more electron-withdrawing pyridyl ring on the amino−imide carbon is expected to have a stronger negative inductive affect on the β-imido nitrogen (decrease of its nucleophilicity) than on the γ-silicon (increase of its electrophilicity), which would generate a net deceleration of the silyl shift for route iii as compared to route iv. Similarly, replacement of a TMS group by the more electron-withdrawing C_6F_5 ring is expected to accelerate the rate of the silyl shift of the remaining TMS for route iv as compared to route ii because of the increase of its electrophilicity.

The TMS shift observed for the 2-pyridyl substituent is therefore a plausible result of its assistance in chelation of the lithium atom in the trans coordination mode. The inhibiting effect of the pentafluorophenyl group on the TMS shift can be explained by two cooperating factors:

i Chelation of the silicon in an NCCF moiety, due to the Si−F strong interactions with the *o*-fluorine of the C_6F_5 ring (routes iii and iv). This interaction reduces the electrophilicity of the silicon atom and also provides some kinetic stability to the silylated amino−imide motif. Similar intramolecular interactions of silicon with various anionic or neutral pendant donors,[6,11,46,47] including organic fluorine,[11,48] are known. Support for this interaction also comes from the room-temperature, silicon-assisted C−F activation in complex **3**[11] and from the solid-state structure of complex **1**, in which the *o*-F···Si distance is 2.956 Å, which is shorter by 0.494 Å than the sum of the van der Waals radii of these atoms. In a toluene solution, at room

Scheme 5. Plausible Mechanism for the Reaction of Complex **1** or $LiNTMS_2 \cdot TMEDA$ with Benzonitrile or 2-Cyanopyridine

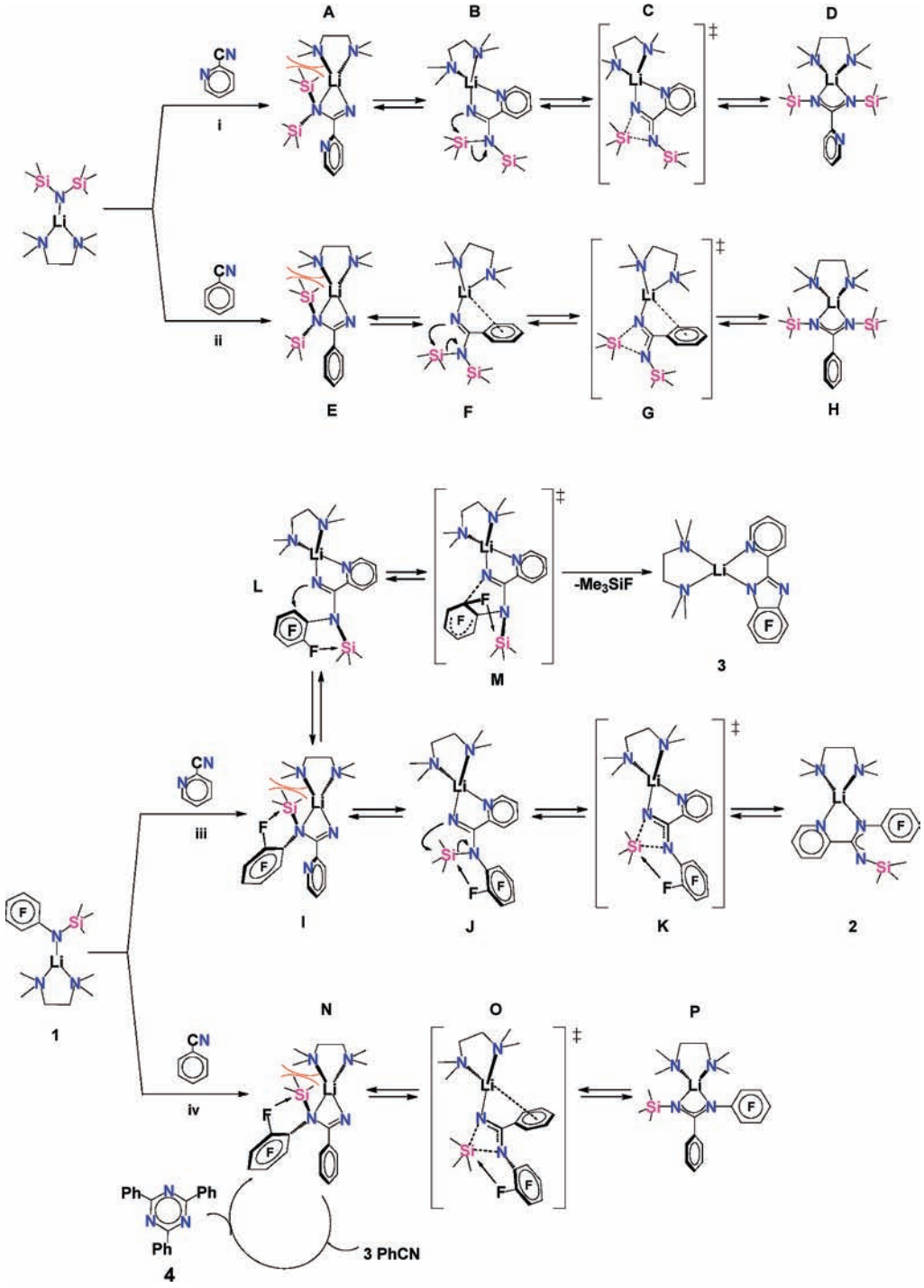

temperature, the hydrogen and carbon signals in the ^{1}H and ^{13}C NMR spectra of both **1** and *N*-(trimethylsilyl)pentafluoroaniline are split,[11,49] as a result of coupling of the *o*-fluorine rings with

(46) (a) Karsch, H. H.; Bienlein, F.; Sladek, A.; Heckel, M.; Burger, K. *J. Am. Chem. Soc.* **1995**, *117*, 5160–5161. (b) Mitzel, N. W.; Losehand, U. *J. Am. Chem. Soc.* **1998**, *120*, 7320–7327. (c) Nakash, M.; Gut, D.; Goldvaser, M. *Inorg. Chem.* **2005**, *44*, 1023–1030. (d) Segmueller, T.; Schlueter, P. A.; Drees, M.; Schier, A.; Nogai, S.; Mitzel, N. W.; Strassner, T.; Karsch, H. H. *J. Organomet. Chem.* **2007**, *692*, 2789–2799. (e) Sidorkin, V. F.; Doronina, E. P. *Organometallics* **2009**, *28*, 5305–5315. (f) So, C.-W.; Roesky, H. W.; Magull, J.; Oswald, R. B. *Angew. Chem., Int. Ed.* **2006**, *45*, 3948–3950.

(47) Kalikhman, I.; Gostevskii, B.; Kingston, V.; Krivonos, S.; Stalke, D.; Walfort, B.; Kottke, T.; Kocher, N.; Kost, D. *Organometallics* **2004**, *23*, 4828–4835.

(48) (a) Bakhtizin, R. Z.; Oreshkin, A. I.; Murugan, P.; Kumar, V.; Sadowski, J. T.; Fujikawa, Y.; Kawazoe, Y.; Sakurai, T. *Chem. Phys. Lett.* **2009**, *482*, 307–311. (b) Fujiki, M.; Saxena, A. *J. Polym. Sci., Part A: Polym. Chem.* **2008**, *46*, 4637–4650. (c) Kawabe, T.; Naito, M.; Fujiki, M. *Polym. J.* **2008**, *40*, 317–326. (d) Kim, S.-Y.; Saxena, A.; Kwak, G.; Fujiki, M.; Kawakami, Y. *Chem. Commun.* **2004**, 538–539. (e) Lousenberg, R. D.; Shoichet, M. S. *J. Org. Chem.* **1997**, *62*, 7844–7849. (f) Mitzel, N. W.; Vojinovic, K.; Froehlich, R.; Foerster, T.; Robertson, H. E.; Borisenko, K. B.; Rankin, D. W. H. *J. Am. Chem. Soc.* **2005**, *127*, 13705–13713. (g) Saxena, A.; Rai, R.; Kim, S.-Y.; Fujiki, M.; Naito, M.; Okoshi, K.; Kwak, G. *J. Polym. Sci., Part A: Polym. Chem.* **2006**, *44*, 5060–5075.

carbon or hydrogen from the TMS methyl. Similar splitting of the signals γ and δ to the perfluorinated phenyl ring are absent from the spectrum of *carbon*-substituted pentafluoroanilides,[50] whereas four-bond coupling constants, $^4J_{FH}$ (H−C−N→Si−F), were observed in fluorosilicon complexes with intramolecular dative Si−N interactions.[47]

ii Strengthening of the Si−N bond β to the C_6F_5 ring. The strengthening of C−C, C−H, and particularly the more polar metal−carbon bonds, mainly due to the negative inductive effect of fluorine, are well documented in both experiment and theory.[51] Because the silicon shift occurs through a concerted rate-determining transition state, the stronger Si−N bond translates to a higher activation barrier for the reaction.

Synthesis, Structure, and Reactivity of the Zirconium Mono- and Tris[tetrafluoro-2-(2-pyridyl)benzimidazolate] Complexes. Synthesis of the Zirconium Benzimidazolate Complexes. Because of our long-standing interest in the study of new group 4 complexes with heteroazaallyl ligands with unique pendant groups, we aimed to synthesize the zirconium and titanium tetrafluoro-2-(2-pyridyl)benzimidazolate complexes. When a solution of 2 equiv of complex **3** is added to a toluene solution of $TiCl_4$, a bright-orange solid precipitates after 30 min. ^{1}H and ^{19}F NMR spectroscopy of a THF-d_8 solution of this solid, which has a negligible solubility in toluene or ether, indicates that it contains a mixture of compounds. These compounds are most likely titanium benzimidazolate complexes, as suggested by the disappearance of the respective lithium benzimidazolate signals from the ^{1}H and ^{19}F NMR spectra. When 2 equiv of complex **3** is added to a toluene suspension of $ZrCl_4$, in an attempt to prepare the zirconium bis(benzimidazolate) complex, the nearly white mixture turns faint bright yellow after 1 h. From this mixture, the tris(benzimidazolate) complex **10** was obtained in an isolated yield of 65% (calculated on the basis of complex **3**), which was slightly improved (to 78%) when stoichiometric amounts of complex **3** and $ZrCl_4$ (3:1) were used (Scheme 6). In an attempt to gain some kinetic control over the ligand substitution process, 2 equiv of complex **3** was reacted with $Zr(NMe_2)_2Cl_2\cdot$ 2THF. However, instead of the expected zirconium bis(benzimidazolate)diamide complex, the mono(benzimidazolate) complex **11** was obtained in an isolated yield of 74% [on the basis of $Zr(NMe_2)_2Cl_2\cdot$2THF; Scheme 6].

Scheme 6. Syntheses of the Zirconium Benzimidazolate Complexes **10** and **11**

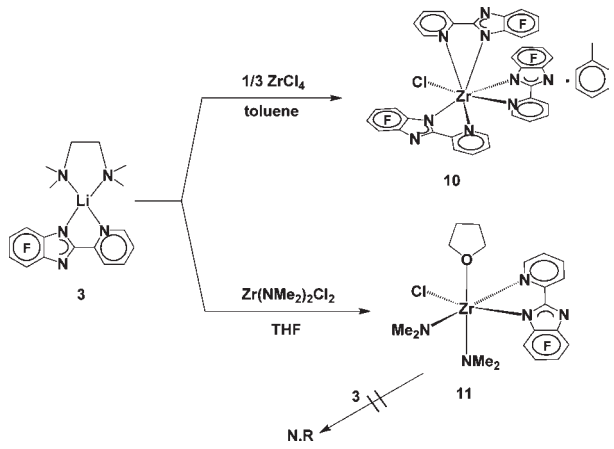

Isolation of complex **11**, which results from the formal substitution of a chloride and a THF ligand in $Zr(NMe_2)_2Cl_2\cdot$2THF with a benzimidazolate ligand, even in the presence of an additional 1 equiv of complex **3**, hints that the salt metathesis stops after replacement of the first chloride with a benzimidazolate ligand (Scheme 6). It is worth mentioning that, unlike the lithium benzimidazolate **5**, the external nitrogen atom, which does not participate in the zirconium NCCN chelation, does not displace a THF ligand or coordinate to the zirconium metal while increasing its coordination number.

Solid-State Structure of the Zirconium Tris(benzimidazolate) Complex 10. Crystallographic data and structure refinement details for complex **10** and selected bond lengths and angles are collected in Tables 1 and 4, respectively. In the solid state, the heptacoordinated zirconium atom in complex **10** adopts a distorted capped-octahedral environment, coordinated to a chlorine atom and to three κ^2-chelating pyridylbenzimidazolate ligands (Figure 5). The Zr−Cl bond makes the "shaft" of "propeller"-shaped, three chelating benzimidazolate ligands, one of which forms a close contact with a toluene solvent molecule through its tetrafluorobenzene ring. The similar distance between the centroids of the toluene and the perfluorocarbon rings in complex **10**, as compared to the centroid−centroid distance found in the C_6F_6/C_6H_6 molecular complex[52] (3.72 and 3.77 Å, respectively), suggests that complex **10** may be considered as a 1:1 molecular complex of toluene and a molecule of zirconium tris(tetrafluorobenzimidazolate) chloride. Interestingly, despite the many conceivable structural isomers, the asymmetric pyridyltetrafluorobenzimidazolate ligands adopt a single mutual arrangement about the zirconium atom.

Whereas all of the three benzimidazolate ligands have similar intramolecular bond lengths and angles, the ligand that interacts with the toluene molecule is differentiated from the other two by its recognizable ligand π-system interaction with the zirconium metal. This difference is evident from comparisons of the degree to which the zirconium atom is displaced from the NCCN plane of the benzimidazole ligands (0.719 Å from the N4−C13−C20−N6 plane, while for the other two ligands,

(49) Oliver, A. J.; Graham, W. A. G. *J. Organomet. Chem.* **1969**, *19*, 17–27.

(50) (a) Bezombes, J. P.; Hitchcock, P. B.; Lappert, M. F.; Merle, P. G. *J. Chem. Soc., Dalton Trans.* **2001**, 816–821. (b) Panda, A.; Stender, M.; Wright, R. J.; Olmstead, M. M.; Klavins, P.; Power, P. P. *Inorg. Chem.* **2002**, *41*, 3909–3916. (c) Vidovic, D.; Findlater, M.; Cowley, A. H. *J. Am. Chem. Soc.* **2007**, *129*, 8436–8437. (d) Wright, R. J.; Steiner, J.; Beaini, S.; Power, P. P. *Inorg. Chim. Acta* **2006**, *359*, 1939–1946.

(51) (a) Clot, E.; Besora, M.; Maseras, F.; Megret, C.; Eisenstein, O.; Oelckers, B.; Perutz, R. N. *Chem. Commun.* **2003**, 490–491. (b) Clot, E.; Megret, C.; Eisenstein, O.; Perutz, R. N. *J. Am. Chem. Soc.* **2009**, *131*, 7817–7827. (c) Evans, M. E.; Burke, C. L.; Yaibuathes, S.; Clot, E.; Eisenstein, O.; Jones, W. D. *J. Am. Chem. Soc.* **2009**, *131*, 13464–13473. (d) Perutz, R. N.; Braun, T. Transition metal-mediated C−F bond activation. In *Comprehensive Organometallic Chemistry III*; Crabtree, R. H., Mingos, D. M. P., Eds.; Elsevier: Oxford, U.K., 2007; pp 725−758.

(52) Williams, J. H. *Acc. Chem. Res.* **1993**, *26*, 593–598.

Table 4. Selected Bond Lengths [Å] and Angles [deg] for Complex **10**

Bond Lengths					
Zr1−N1	2.191(4)	N1−C2	1.392(6)	N7−C26	1.387(7)
Zr1−N4	2.230(4)	N2−C1	1.321(6)	N8−C25	1.359(6)
Zr1−N8	2.237(4)	N2−C7	1.399(6)	N8−C31	1.385(6)
Zr1−N3	2.363(4)	N4−C13	1.372(6)	C1−C8	1.443(6)
Zr1−N9	2.363(4)	N4−C14	1.374(6)	C13−C20	1.464(7)
Zr1−Cl1	2.4113(16)	N5−C13	1.320(6)	C25−C32	1.456(7)
Zr1−N6	2.434(4)	N5−C19	1.382(6)		
N1−C1	1.374(6)	N7−C25	1.326(6)		

Bond and Torsion Angles			
N1−Zr1−N4	134.04(14)	N1−Zr1−N6	136.85(15)
N1−Zr1−N8	79.53(14)	N4−Zr1−N6	68.65(14)
N4−Zr1−N8	143.87(15)	N8−Zr1−N6	76.86(14)
N1−Zr1−N3	69.72(14)	N3−Zr1−N6	84.89(14)
N4−Zr1−N3	78.45(14)	N9−Zr1−N6	73.96(14)
N8−Zr1−N3	109.46(14)	Cl1−Zr1−N6	141.34(10)
N1−Zr1−N9	129.91(14)	Zr1−N4−C13−N5	15.72
N4−Zr1−N9	89.22(14)	Zr1−N6−C20−C21	20.26
N8−Zr1−N9	70.79(14)	N4−C13−C20−N6	2.61
N3−Zr1−N9	158.31(14)	Zr1−N1−C1−N2	4.66
N1−Zr1−Cl1	81.76(12)	Zr1−N3−C8−C9	2.86
N4−Zr1−Cl1	85.28(12)	N1−C1−C8−N3	0.45
N8−Zr1−Cl1	117.65(11)	Zr1−N8−C25−N7	6.83
N3−Zr1−Cl1	118.28(11)	Zr1−N9−C32−C33	3.34
N9−Zr1−Cl1	77.79(11)	N8−C25−C32−N9	1.60

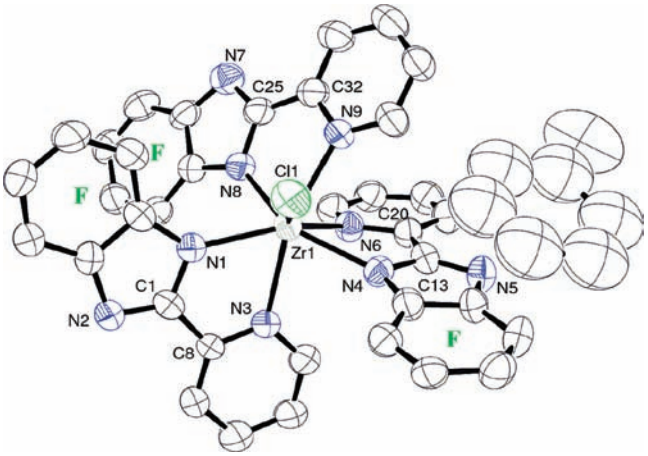

Figure 5. ORTEP diagram of the molecular structure of complex **10** (50% thermal ellipsoids). Hydrogen and fluorine atoms are omitted for clarity (the tetrafluorophenylene ring is marked with an "F").

this distance is 0.192 and 0.151 Å). Additionally, there is a notable bending of the C−C bond of the N4 benzimidazolate ligand, as evidenced by a dihedral angle of 11.49° between the pyridyl and benzimidazolyl rings. Interestingly, in the benzimidazolate ligand forming the motif Zr−N6−C20−N4, both nitrogen atoms are partially π-bonded. However, when the Zr−N6 and Zr−N4 bond lengths are compared, the former is longer by 0.08 Å, whereas the Zr−N4 bond is similar to those of the other benzimidazolate ligands. This difference in bond lengths can be rationalized by the involvement of the electron-rich azaallyl moiety N4−C13−N5 as compared to that of the pyridyl system.

Solid-State Structure of the Zirconium Mono(benzimidazolate) Complex 11. Crystallographic data and structure refinement details for complex **11** and selected bond lengths and angles are collected in Tables 1 and 5, respectively. In the solid state, complex **11** crystallizes as two independent structural isomers (**11A** and **11B** in 23% and 77% occupancy, respectively; Figure 6). These two overlapping molecules are predominantly distinguished by the different extent of the slippage of the central octahedral zirconium atom from the plane of the chelating tetrafluoro-2-(2-pyridyl)benzimidazolate ligand. The dimethylamido, THF, and chloride ligands in complex **11** retain their relative positions as in the structure of $Zr(NMe_2)_2Cl_2 \cdot 2THF$,[53] i.e., two *cis*-$NMe_2$ ligands and THF and chloride ligands, which are trans and cis, respectively, to one of the NMe_2 ligands. The κ^2-tetrafluoro-2-(2-pyridyl)benzimidazolate ligand is bonded to the positions trans to the chloride and second NMe_2 ligands with the benzimidazolate and pyridyl moieties, which replaces the Zr−Cl and "dative" Zr−O bonds, respectively, in $Zr(NMe_2)_2Cl_2 \cdot 2THF$. The two occupation sites of the zirconium atom in the overlapping complexes **11A** and **11B** are ca. 1 Å apart and roughly inline with respect to the O1−N2 axis [the O1−Zr1A−N2 and N2−Zr1B−O1 angles are 165.4(3)° and 165.6(3)°, respectively]. In both of the structures, a noticeable slippage of the zirconium metal from the pyridylbenzimidazolate ligand is observed (the deviations from the NCCN plane by Zr1A and Zr1B are 0.671 and 0.348 Å, respectively).

It is worth noting that, in both complexes **10** and **11**, the first structurally characterized zirconium benzimidazolates, particularly in the latter, a noticeable tendency of the zirconium metal toward an interaction with the ligand π system was observed (probably in both cases because of packing forces), a common bonding mode for the closely related amidinates.

Behavior of the Zirconium Mono- and Tris[tetrafluoro-2-(2-pyridyl)benzimidazolate] Complexes 10 and 11 in the Polymerization of Propylene. The addition of methyl

(53) Brenner, S.; Kempe, R.; Arndt, P. *Z. Anorg. Allg. Chem.* **1995**, *621*, 2121–2124.

Table 5. Selected Bond Lengths [Å] and Angles [deg] and for Complex **11**

Bond Lengths					
Zr1A···Zr1B	1.022(6)	Zr1A−Cl1	2.474(3)	Zr1B−Cl1	2.496(2)
Zr1A−O1	1.391(13)	Zr1B−O1	2.402(10)	N3−C11	1.370(7)
Zr1A−N1	2.199(9)	Zr1B−N1	2.036(6)	N5−C11	1.312(7)
Zr1A−N2	2.900(13)	Zr1B−N2	1.890(9)	C11−C12	1.465(8)
Zr1A−N3	2.391(6)	Zr1B−N3	2.297(5)		
Zr1A−N4	2.473(6)	Zr1B−N4	2.452(5)		

Bond and Torsion Angles			
O1−Zr1A−N1	116.4(4)	N3−Zr1B−O1	76.4(2)
O1−Zr1A−N2	165.4(3)	N2−Zr1B−N4	89.7(3)
O1−Zr1A−N3	96.9(3)	N1−Zr1B−N4	162.7(3)
N1−Zr1A−N3	93.9(3)	N3−Zr1B−N4	69.69(17)
O1−Zr1A−N4	97.6(3)	O1−Zr1B−N4	76.1(2)
N1−Zr1A−N4	143.5(5)	N2−Zr1B−Cl1	99.1(2)
N3−Zr1A−N4	67.89(19)	N1−Zr1B−Cl1	98.3(2)
O1−Zr1A−Cl1	109.9(3)	N3−Zr1B−Cl1	150.16(17)
N1−Zr1A−Cl1	94.7(2)	O1−Zr1B−Cl1	82.32(15)
N3−Zr1A−Cl1	144.4(3)	N4−Zr1B−Cl1	85.17(13)
N4−Zr1A−Cl1	85.20(17)	N5−C11−N3	117.5(5)
N2−Zr1B−N1	106.4(4)	N3−C11−C12−N4	3.45
N2−Zr1B−N3	96.7(3)	Zr1A−N4−C13−N5	17.03
N1−Zr1B−N3	101.3(2)	Zr1A−N4−C12−C16	20.18
N2−Zr1B−O1	165.6(3)	Zr1B−N4−C13−N5	11.32
		Zr1B−N4−C12−C16	6.71

aluminoxane (MAO; 1:1000 Zr/Al molar ratio) to a toluene solution of complex **10** or **11** results in no significant color change. Whereas the solution of complex **10** showed only negligible activity in the polymerization of liquefied propylene, complex **11** gave a sticky polymer in a modest activity of 6.99×10^4 [g/mol·h]. This hexane-soluble polymer has a low tacticity and molecular weight (mmmm % = 9.5 and M_n = 3000, respectively) and a high polydispersity (M_w/M_n = 4.4). These results imply that the tris- and mono(benzimidazolate) complexes are not converted during the polymerization process to common active species, as was observed for the titanium bis- and mono(benzamidinate)s.[54] Further, the pendant 3- and 6-fluorine atoms do not participate in the termination-hindering interaction with the growing polymer chain and the polymerization is neither single-site nor living.[55]

Conclusions

There are marked differences between the reactivity of $LiNTMS_2 \cdot TMEDA$ or **1** toward aromatic nitriles. Whereas amidinates are the major products of the reaction of $LiNTMS_2 \cdot TMEDA$ with all of the examined nitriles except for C_6F_5CN in THF, complex **1** showed a diverse chemoselectivity in its reactions: no reaction with *o*-$OMeC_6H_4CN$, trimerization of benzonitrile to triazine, nucleophilic aromatic attack with C_6F_5CN in both ether or THF, and production of amidinate and subsequently benzimidazolate (**3**) with 2-cyanopyridine. From the reaction of complex **1** and C_6F_5CN, a unique, hexacoordinate lithium coordination polymer was obtained. This lesser activity and different reaction paths taken by complex **1** in its reactions with nitriles as compared to $LiNTMS_2 \cdot TMEDA$ seems to be affected by the electrophilicity of the nitrile, by the availability of adequate pendant group for the chelation of the lithium metal during the reaction, and by three unique effects of the pentafluorophenyl ring: strengthening of the Si−N bond, decreasing of the nitrogen nucleophilicity, and interaction of the *o*-fluorine and silicon atoms. In addition, zirconium mono- or tris[tetrafluoro-2-(2-pyridyl)benzimidazolate] were prepared from the reaction of complex **3** and $Zr(NMe_2)_2Cl_2 \cdot 2THF$ or $ZrCl_4$, respectively. In these complexes, the first synthesized zirconium mono- and tris(benzimidazolate)s, the benzimidazolate ligand has a distinct tendency toward π bonding with the zirconium metal. When activated by MAO, only the mono(benzimidazolate) complex showed modest activity in the polymerization of propylene. Synthetic attempts to produce the bis(perfluorinated benzimidazolate) complexes are in progress toward their study in the stereoregular polymerization and copolymerization of α-olefins.

Experimental Section

General Procedures. All manipulations of air-sensitive materials were carried out with the rigorous exclusion of oxygen and moisture in an oven-dried or flamed Schlenk-type glassware on a dual-manifold Schlenk line or interfaced to a high-vacuum (10^{-5} Torr) line or in a nitrogen-filled glovebox (M. Braun) with a medium-capacity recirculator (1−2 ppm O_2). Argon and nitrogen were purified by passage through a MnO oxygen-removal column and a Davison 4 Å molecular sieve column. Analytically pure solvents were distilled under nitrogen from potassium benzophenone ketyl (THF), sodium (toluene and TMEDA), and Na/K alloy (ether, hexane, toluene-d_8, and THF-d_8). Complexes **1**, **3**, and **9**[11] and $Zr(NMe_2)_2Cl_2 \cdot 2THF$[53] were synthesized according to literature procedures. Nitriles (Aldrich) were degassed, and $ZrCl_4$ (Aldrich) was sublimed under reduced pressure prior to use.

NMR spectra were recorded on Bruker Avance 300 and 500 spectrometers. ^1H and ^{13}C chemical shifts are referenced to internal solvent resonances and reported relative to TMS. ^{19}F and ^7Li chemical shifts were referenced according to IUPAC recommendations.[56] The experiments were conducted in Teflon-sealed NMR tubes (J. Young) after the preparation of the

(54) Volkis, V.; Lisovskii, A.; Tumanskii, B.; Shuster, M.; Eisen, M. S. *Organometallics* **2006**, *25*, 2656–2666.

(55) (a) Sakuma, A.; Weiser, M.-S.; Fujita, T. *Polym. J.* **2007**, *39*, 193–207. (b) Makio, H.; Fujita, T. *Bull. Chem. Soc. Jpn.* **2005**, *78*, 52–66. (c) Furuyama, R.; Saito, J.; Ishii, S.; Makio, H.; Mitani, M.; Tanaka, H.; Fujita, T. *J. Organomet. Chem.* **2005**, *690*, 4398–4413.

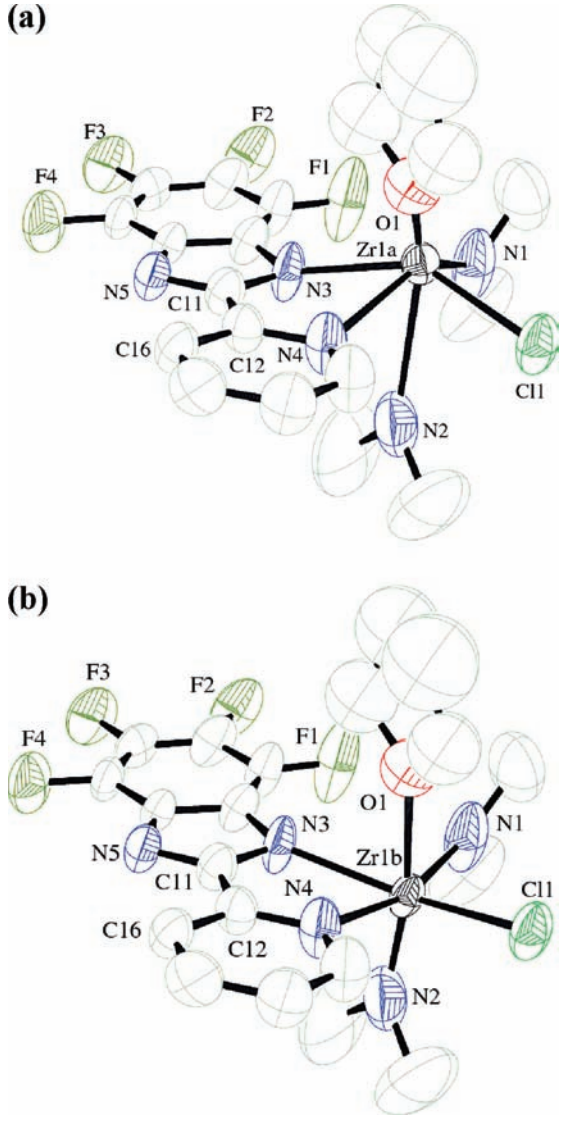

Figure 6. ORTEP diagram of the molecular structure of complexes **11A** (a) and **11B** (b) (50% thermal ellipsoids). Hydrogen atoms are omitted for clarity.

sample under anaerobic conditions, with dried toluene-d_8 or THF-d_8. The molecular weights and polydispersities of the polymers were determined by the gel permeation chromatography (GPC) method on a Varian PL-GPC 220 instrument using 1,2,4-trichlorobenzene as the mobile phase at 160 °C. Polystyrene standards were used for the standard calibration curve of GPC.

X-ray Crystallographic Measurements. The single-crystalline material was immersed in parathone-N oil and was quickly fished with a glass rod and mounted on a Kappa CCD diffractometer under a cold stream of nitrogen. Data collection was performed using monochromatized Mo Kα radiation using φ and ω scans to cover the Ewald sphere.[57] Accurate cell parameters were obtained with the amount of indicated reflections (Table 1).[58] The structure was solved by *SHELXS-97* direct methods[59] and refined by the *SHELXL-97* program package.[60] The atoms were refined anisotropically. Hydrogen atoms were included using the riding mode. Software used for molecular graphics: *ORTEP, TEXSAN Structure Analysis Package*.[61] The cell parameters and refinement data are presented in Table 1.

Syntheses. General Procedure for the Reaction of ($Me_3SiNC_6F_5$)Li·TMEDA (1) with Nitriles. A certain amount of complex **1** was charged in the glovebox into a swivel frit equipped with two 100 mL flasks. After the frit was connected to a high-vacuum line, 30 mL of toluene or THF was added, the resulting solution was cooled to 0 °C, and an equimolar amount of the corresponding nitrile was added dropwise using a syringe. The cooling bath was removed, the resulting solution was stirred at room temperature for 2 h and then filtered, and the volatiles were evaporated from the filtrate until turbidity was noted. The concentrated filtrate was cooled to −50 °C, and the formed solids were separated from the mother liquor by fast filtration or decantation, washed with small amounts of cold hexane, and dried with a stream of argon.

Synthesis of Triphenyl-1,3,5-triazine (4). A total of 1.888 g (4.85 mmol) of complex **1** and 0.500 g (4.85 mmol) of benzonitrile gave 0.336 g (67% yield) of **4**. This previously published compound[13] was identified by ^{1}H NMR and X-ray analysis. It is important to add that catalytic amounts of complex **1** with benzonitrile will also produce the same trimer but in a less efficient manner.

Synthesis of $\{[C_6F_4N_2C(2\text{-}C_5H_4N)]Li\cdot THF\}_n$ (5). A total of 1.869 g (4.8 mmol) of complex **1** and 0.500 g (4.8 mmol) of 2-cyanopyridine gave 1.342 g (78% yield) of **5**. ^{1}H NMR (300 MHz, THF-d_8): δ 8.522 (br m, 1H, py-H_6), 8.465 (td, J_1 = 7.9 Hz, J_2 = 1.2 Hz, 1H, py-H_3), 7.887 (dt, J_1 = 8.0 Hz, J_2 = 1.4 Hz, 1H, py-H_5), 7.351 (t, ^3J = 7.9 Hz, 1H, py-H_4), 3.614 (m, OCH_2), 3.577 (s, OC*H*D), 1.771 (m, OCH_2CH_2), 1.725 (s, OCD_2CHD). ^{19}F NMR (188 MHz, THF-d_8): δ −160.685 (br s, 2F, *o*-F), −175.710 (br s, 2F, *m*-F). ^{7}Li NMR (194.4 MHz, THF-d_8): δ −1.7975. ^{13}C NMR (76.5 MHz, THF-d_8): δ 162.92 (s, 1C, NCN), 155.71 (s, 1C, py-C_2), 149.13 (s, 1C, py-C_6), 138.11 (s, 1C, py-C_4), 138.17 (m, $^1J_{CF}$ = 243.2 Hz, 2C, *o*-C−F), 135.38 (m, $^1J_{CF}$ = 239.8 Hz, 2C, *m*-C−F), 133.09 (m, 2C, C−N), 122.84 (s, 1C, py-C_5), 122.54 (s, 1C, py-C_3), 67.31 (q, OCD_2), 66.33 (s, OCH_2), 26.38 (s, OCH_2CH_2), 25.32 (q, OCD_2CD_2). Anal. Calcd for $C_{16}H_{12}F_4LiN_3O$ (345.22): C, 55.67; H, 3.50; F, 22.01; N, 12.17. Found: C, 47.68; H, 3.43; F, 24.31; N, 11.09.

Synthesis of $[LiN(4\text{-}CN\text{-}2,3,5,6\ tetrafluorophenyl)(C_6F_5)\cdot THF\cdot TMEDA]_n$ (7). A total of 2.017 g (5.2 mmol) of complex **1** and 1.000 g (5.2 mmol) of pentafluorobenzonitrile gave 2.548 g (87% yield) of **5**. ^{1}H NMR (300 MHz, THF-d_8): δ 3.576 (s, OC*H*D), 2.300 (s, 4H, CH_2N), 2.146 (s, 12H, CH_3N), 1.725 (s, OCD_2CHD). ^{19}F NMR (282.4 MHz, THF-d_8): δ −147.115 (m, $^3J_{FF}$ = 14.7 Hz, 2F, N−CC*F*), −158.316 (m, $^3J_{FF}$ = 20.8 Hz, 2F, *o*-F), −166.491 (m, $^3J_{FF}$ = 14.7 Hz, 2F, NC−CC*F*), −172.417 (t, $^3J_{FF}$ = 20.8 Hz, 2F, *m*-F), −177.763 (m, $^3J_{FF}$ = 20.8 Hz, 1F, *p*-F). ^{13}C NMR (75.4 MHz, THF-d_8): δ 148.74, (m, $^1J_{CF}$ = 242.3 Hz, 2C, N−C*C*F), 142.59 (m, $^1J_{CF}$ = 225.7 Hz, 2C, *o*-C−F), 141.42, (m, $^1J_{CF}$ = 221.5 Hz, 2C, NC−C*C*F), 139.54 (m, $^1J_{CF}$ = 234.1 Hz, 2C, *m*-C−F), 136.67 (m, 1C, C−N), 134.64 (m, $^1J_{CF}$ = 240.2 Hz, 1C, *p*-C−F), 112.15 (t, $^3J_{CF}$ = 3.5 Hz, 1C, C−CN), 67.45 (q, OCD_2), 58.85 (CH_2N), 46.23 (CH_3N), 25.32 (q, OCD_2-CD_2). Anal. Calcd for $C_{23}H_{24}F_9LiN_4O$ (550.39): C, 50.19; H, 4.40; F, 31.07; N, 10.18. Found: C, 49.13; H, 3.56; F, 24.10; N, 8.86.

Synthesis of $[C_6F_4N_2C(2\text{-}C_5H_4N)]_3ZrCl\cdot C_7H_8$ (10). To a swivel frit equipped with 100 mL flasks was added inside the glovebox 0.400 g (1.71 mmol) of $ZrCl_4$. The frit was connected to a high-vacuum line, and the solids were suspended in 25 mL of toluene, which was cooled to 0 °C. A total of 2.000 g (5.14 mmol)

(56) Harris, R. K.; Becker, E. D.; Cabral De Menezes, S. M.; Goodfellow, R.; Granger, P. *Pure Appl. Chem.* **2001**, *73*, 1795–1818.
(57) *Kappa CCD Server Software*; Nonius BV: Delft, The Netherlands, 1997.
(58) Otwinowski, Z.; Minor, W. *Methods Enzymol.* **1997**, *276*, 307.
(59) Sheldrick, G. M. *Acta Crystallogr., Sect. A: Found. Crystallogr.* **1990**, *A46*, 467.
(60) *ORTEP, TEXSAN Structure Analysis Package*; Molecular Structure Corp., MSC: The Woodlands, TX, 1999.
(61) Sheldrick, G. M. *SHELXL97, Program for the Refinement of Crystal Structures*; University of Gottingen: Gottingen, Germany, 1997.

of complex **3** was dissolved in 20 mL of toluene, and the solution was injected dropwise to the frit. The faint-yellow suspension that resulted was stirred for 3 h, after which the reaction mixture was evaporated and TMEDA was removed by low-pressure azeotrope distillations with toluene. The resulting solids were extracted with hot toluene (ca. 50 °C, 3 × 25 mL), and the extract was filtered. The volume of the filtrate was reduced to half, and the concentrated solution was cooled gradually to −4 °C for 72 h to yield bright-yellow crystals of the product. The crystals were separated from the mother liquor by decantation, washed twice with a small amount of cold hexane, and dried with a gentle stream of argon (1.359 g, 78% yield). ^{1}H NMR (300 MHz, THF-d_8): δ 8.675 (ddd, ^3J = 4.8 Hz, ^4J = 1.7 Hz, ^5J = 1.0 Hz,1H, py-H$_6$), 8.425 (td, ^3J = 7.9 Hz, ^4J = ^5J = 1.0 Hz, 1H, py-H$_3$), 7.939 (dt, ^3J = 7.7 Hz, ^4J = 1.8 Hz, 1H, py-H$_4$), 7.456 (ddd, ^3J = 7.6 and 4.8 Hz, ^4J = 1.2 Hz, 1H, py-H$_5$), 3.577 (s, OC*H*D), 1.725 (s, OCD$_2$C*H*D). ^{19}F NMR (188 MHz, THF-d_8): δ −162.763 (br s, 2F, *o*-F), −164.554 (br s, 2F, *m*-F). ^{13}C NMR (76.5 MHz, THF-d_8): δ 159.91 (s, 1C, NCN), 151.13 (s, 1C, py-C$_2$), 147.66 (s, 1C, py-C$_6$), 136.94 (s, 1C, py-C$_4$), 122.45 (s, 1C, py-C$_5$), 122.04 (s, 1C, py-C$_3$), 67.35 (q, O*C*D$_2$), 25.32 (q, OCD$_2$*C*D$_2$). Anal. Calcd for $C_{43}H_{20}ClF_{12}N_9Zr$ (1017.34): C, 50.77; H, 1.98; N, 12.39. Found: C, 49.53; H, 2.29; N, 11.86.

Synthesis of [C$_6$F$_4$N$_2$C(2-C$_5$H$_4$N)](NMe$_2$)$_2$ZrCl·THF (11). To a swivel frit equipped with 100 mL flasks was added inside the glovebox 1.013 g (2.57 mmol) of Zr(NMe$_2$)$_2$Cl$_2$·2THF. The frit was connected to a high-vacuum line, and the solids were dissolved in 20 mL of THF, which was cooled to 0 °C. A total of 1.000 g (2.57 mmol) of complex **3** was dissolved in 15 mL of THF, and the solution was injected dropwise to the frit. The off-white suspension that resulted was stirred for 3 h, after which the reaction mixture was evaporated and TMEDA was removed by low-pressure azeotrope distillations with toluene. The resulting solids were extracted with toluene (2 × 25 mL), and the extract was filtered. The filtrate was evaporated until saturation, and the concentrated solution was cooled gradually to −35 °C for 96 h to yield faint-yellow crystals of the product. The crystals were separated from the mother liquor by filtration, washed twice with a small amount of cold hexane, and dried carefully under vacuum (1.052 g, 74% yield). ^{1}H NMR (200 MHz, THF-d_8): δ 8.494 (br m, 1H, py-H$_6$), 8.462 (m, 1H, py-H$_3$), 7.853 (dt, ^3J = 8.1 Hz, ^4J = 1.5 Hz, 1H, py-H$_4$), 7.294 (ddd, ^3J = 7.4 and 4.9 Hz, ^4J = 1.3 Hz, 1H, py-H$_5$), 3.626 (m, OCH_2), 3.575 (s, OC*H*D), 3.055 (s, 6H, NMe$_2$), 3.047 (s, 6H, NMe$_2$), 1.775 (m, OCH$_2$CH_2), 1.725 (s, OCD$_2$C*H*D). ^{19}F NMR (188 MHz, THF-d_8): δ −160.494 (br s, 2F, *o*-F), −175.671 (dd, $^3J_{FF}$ = 14.0 and 11.5 Hz, 2F, *m*-F). ^{13}C NMR (75.5 MHz, THF-d_8): δ 163.80 (s, 1C, NCN), 147.18 (s, 1C, py-C$_2$), 145.19 (s, 1C, py-C$_6$), 139.81 (s, 1C, py-C$_4$), 122.97 (s, 1C, py-C$_5$), 122.89 (s, 1C, py-C$_3$), 67.38 (q, O*C*D$_2$), 66.31 (s, O*C*H$_2$), 45.85 (s, 2C, NMe$_2$), 45.61 (s, 2C, NMe$_2$), 26.33 (s, OCH$_2$*C*H$_2$), 25.32 (q, OCD$_2$*C*D$_2$). Anal. Calcd for $C_{20}H_{24}ClF_4N_5OZr$ (553.11): C, 43.43; H, 4.37; N, 12.66. Found: C, 46.36; H, 3.17; N, 11.79.

Propylene Polymerization Experiments with Complexes 10 and 11. In a glovebox, a 3 mL toluene solution of 46.5 μmol of the catalyst (47.4 or 32.4 mg of complexes **10** or **11**, respectively) was added to a solution of 2.700 g of MAO in 15 mL of toluene, followed by stirring with a glass rod. The resulting solution was equally divided into three parts, each of which was transferred to a 100 mL beaker equipped with a stir bar. The beakers were placed in steel reactors that were then connected to a high-vacuum line, cooled to liquid-nitrogen temperature, and pumped down. A total of 35 mL of liquid propylene was vacuum transferred to each of the reactors. The temperature was then raised to 25 °C using a thermostatted bath, and the stirring began. After 3 h, the unreacted propylene was exhausted in a hood and the reaction mixture was quenched by the addition of 30 mL of acetylacetone (acac). The polymer was separated from the organic phase, cut down to small pieces, extracted for 2 days with methanol and then acetone to remove traces of Al(acac)$_3$, acac, and toluene, and dried under vacuum at 50 °C. No soluble polymeric fractions were found in the organic washing solvents.

Acknowledgment. This research was supported by the USA−Israel Binational Science Foundation under Contract 2008283. S.A. thanks Raymond Rosen for his fellowship.

Supporting Information Available: Figures of the extended structures of polymers **5** and **7** and X-ray crystallographic data in CIF format for complexes **5**, **7**, **10**, and **11**. This material is available free of charge via the Internet at http://pubs.acs.org.